Eur J Nucl Med Mol Imaging (2017) 44:41–49
DOI 10.1007/s00259-016-3469-3

ORIGINAL ARTICLE

Evaluation of bone-seeking novel radiotracer ^{68}Ga-NO2AP-Bisphosphonate for the detection of skeletal metastases in carcinoma breast

Averilicia Passah[1] · Madhavi Tripathi[1] · Sanjana Ballal[1] · Madhav Prasad Yadav[1] · Rajeev Kumar[1] · Frank Roesch[2] · Marian Meckel[2] · Partha Sarathi Chakraborty[1] · Chandrasekhar Bal[1]

Received: 30 May 2016 / Accepted: 14 July 2016 / Published online: 25 July 2016

Abstract
Purpose The successful labelling of bisphosphonates (BP) with ^{68}Ga using macrocyclic chelators such as the based triazacyclononane (NO2AP) is a step forward in the in-house availability of a novel bone-seeking PET radiopharmaceutical with dual advantage of PET/CT imaging and generator production. In this study, we compared the novel generator-based skeletal radiotracer ^{68}Ga-1,4,7-triazacyclonone-1,4-diacetic acid (^{68}Ga-NO2AP-BP) with sodium fluoride (^{18}F-NaF) for the detection of skeletal metastases in breast cancer patients. In addition, dosimetric analysis of ^{68}Ga-NO2AP-BP was performed in a subset of patients.
Methods This was a prospective study of histopathologically proven cases of breast cancer patients who were referred for bone scintigraphy and underwent positron emission tomography/computed tomography (PET/CT) with ^{18}F-NaF and ^{68}Ga-NO2AP-BP within a week in random order. The scans of each patient were compared both qualitatively for image quality and quantitatively for number of lesions and SUVmax of lesions. Dosimetric analysis was performed in five patients. Their PET/CT scans were acquired at multiple time points and urine and blood samples were collected. Dosimetric calculations were performed using OLINDA/EXM 1.1 software. Statistical analysis was done using Stata 13 (StataCorp) software package. An agreement analysis regarding number of lesions detected with the two skeletal radiotracers was carried out.
Results The image quality of ^{68}Ga-NO2AP-BP PET/CT scans were comparable to that of ^{18}F-NaF. There was no statistically significant difference in the SUVmax of lesions, normal bone and lesion to background ratio between the two skeletal radiotracers. There was good agreement in the number of lesions detected by both skeletal radiotracers. The mean whole body effective dose for ^{68}Ga-NO2AP-BP was 0.00583 mSv/MBq and the effective dose equivalent was 0.0086 mSv/MBq.
Conclusion The excellent lesion detection agreement between ^{68}Ga-NO2AP-BP and ^{18}F-NaF favours the former as an alternative for skeletal scintigraphy in centres without an on-site cyclotron. The favourable dosimetric results and its potential to be used as a theranostic agent makes it an important generator-based skeletal radiotracer.

Keywords Breast cancer · Positron emission tomography · ^{18}F-Sodium Fluoride · ^{68}Ga-1,4,7-triazacyclonone-1,4-diacetic acid

Introduction

Skeletal scintigraphy using ^{18}F-sodium fluoride (^{18}F-NaF) has proven superior to the conventional ^{99m}Tc-phosphonate bone scan, in particular because of the use of positron emission tomography/computed tomography (PET/CT) technology, which offers a higher sensitivity and spatial resolution along with routine CT acquisition, thus improving specificity of lesions detected [1, 2]. While ^{18}F-NaF is cyclotron produced, PET radionuclide generator systems like ^{68}Ge/^{68}Ga generator serve as instant sources of short-lived radionuclides in institutions not equipped with an onsite cyclotron. The successful

✉ Chandrasekhar Bal
csbal@hotmail.com

[1] Department of Nuclear Medicine, All India Institute of Medical Sciences, Ansari Nagar, New Delhi 110029, India

[2] Nuclear Chemistry, Johannes-Gutenberg-University, Mainz, Germany

labelling of bisphosphonates (BP) with ^{68}Ga using macrocyclic chelators such as DOTA is a step forward in the in-house availability of a novel bone-seeking PET radiopharmaceutical with dual advantage of PET/CT imaging and generator production. Pre-clinical studies have further reported alpha amino propionic acid-based 1,4,7 triazacyclononane) [3, 4], in particular ^{68}Ga-NO2AP-BP, to have excellent tumour to background ratio and to facilitate imaging of small bone metastases [5]. As ^{18}F-NaF is the agent with the highest sensitivity and specificity for evaluating skeletal metastases in breast cancer [6–9], in this prospective study, the primary objective was to compare head-to-head ^{68}Ga-NO2AP-BP and ^{18}F-NaF PET/CT for the detection of skeletal metastases in breast carcinoma patients. A secondary objective was to perform dosimetric analysis of ^{68}Ga-NO2AP-BP as a new skeletal radiotracer.

Materials and methods

This was a prospective single centre study to compare the novel skeletal radiotracer ^{68}Ga-NO2AP-BP with the reference standard ^{18}F-NaF for skeletal PET/CT imaging. Figure 1 illustrates the structures of NO2AP-BP and (4-{bis-(phosphonomethyl)carbamoyl]methyl}-7,10-bis)carboxymethyl)-1,4,7,10-tetraazacyclododec-1-yl)acetic acid (BPAMD). Breast cancer was chosen for the study as both osteoblastic and osteolytic lesions can occur and we can compare the localisation of the two skeletal PET tracers in both types of lesions. The study was approved by the Institute Ethics Committee (IESC/T-236/15.06.2013), and written informed consent was taken from each patient before inclusion.

Patient characteristics

Inclusion and exclusion criteria

Pathologically proven breast carcinoma patients who underwent ^{99m}Tc-methylene diphosphonate (^{99m}Tc-MDP) skeletal scintigraphy were recruited for the study. Patients with one or more sites of abnormal tracer accumulation on the ^{99m}Tc-MDP bone scan which were suspicious for metastases were mainly focused. Pregnant and lactating female patients were excluded. Patients who refused to give informed consent were also excluded from the study.

As reported in the literature, 5–6 % of breast cancer patients [10] progress to skeletal metastases, and taking 10 % clinical error, a sample size of 22 patients was required to conduct the study. However, in the current study we have successfully analysed 28 patients.

Methods

Sample size and place of study

The study included 28 patients and was conducted between 2013 and 2015 in the Department of Nuclear Medicine, AIIMS, New Delhi.

Synthesis of ^{68}Ga-NO2AP-BP

^{68}Ga-NO2AP-BP was synthesised as described in detail by Holub et al. [5]. $^{68}Ga^{3+}$ was obtained from the ^{68}Ge/^{68}Ga generator and complexed with the bisphosphonate as detailed below. ^{68}Ga was eluted as cation from a 1850 MBq (50 mCi) ^{68}Ge/^{68}Ga generator (Isotope Technology Garching GmbH, Germany) with 5–7 ml of 0.05 M HCl (elution yield is ~80 %). Following the standard protocol from Mainz [11], this eluate was then passed through a cation exchange resin strata (X-C phenomenex) online, which removed impurities and pre-concentrated the generator eluate. ^{68}Ga was adsorbed onto the cartridge and the whole eluate solution passed into the waste. N2 solution (400 μl mixture of 97.6 % acetone and 0.05 N HCl) was used to release concentrated and purified ^{68}Ga from the strata X-C. ^{68}Ga was delivered into the reaction vial that contained the precursor NO2AP (20 μg dissolved in 1.5 mL 0.25 M sodium acetate). The reaction vessel was heated for 15 min at 95 °C. After heating, the labelled product was allowed to cool down. For purification purposes, the product was diluted with 5 ml of sterile water and passed through a STRATA X-C cartridge where the free Gallium was trapped on the resin and the pure labelled ^{68}Ga-NO2AP-BP was present in the solution. The product was diluted with saline and

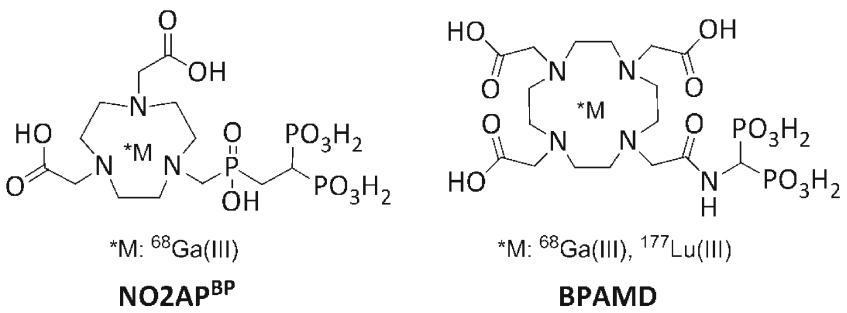

Fig. 1 Structures of NO2AP-BP and BPAMD

was made sterile by passing through a 0.22 μm millipore filter. All synthesis steps were carried out in an automated module (Modular lab, Eckert and Ziegler, Germany). The total synthesis time was 18 min. For each run, a routine quality control test was performed with the help of radio-TLC, pH paper and dose calibrator. Labelling efficiency achieved in each synthesis was > 98 %.

Synthesis of ^{18}F-NaF

The detailed procedure for synthesis and purification ^{18}F-NaF has been described by our centre [12]. In brief, ^{18}O water was irradiated by protons to produce ^{18}F ions in an 11 MeV RDS 111 Medical Cyclotron (Siemens). ^{18}F was transferred from the target to trap and release the column of the Explora FDG-4 module through the V-vial. Residual ^{18}F in the V-vial was transferred to the second Explora module and ^{18}F fluoride ion was trapped in the trap and release column. The trap and release column removes the silver content coming from the silver target. Trapped ^{18}F fluoride ion was eluted with eluting agent (mixture of K222, K_2CO_3, water and acetonitrile) and transferred to a sterile empty vial in the hot cell through reaction vessels after filtering through a Millipore Milex 0.22 μm GS vented filter. Cation exchange resin was used for removal of K222. Dilution was done with normal saline (0.9 % NS) to form ^{18}F-NaF. Mean total purification time was 8 min. Quality control was done as per United State Pharmacopia (USP) guidelines.

Study protocol

Patients who fulfilled inclusion criterion underwent ^{18}F-NaF and ^{68}Ga-NO2AP-BP PET/CT in random fashion were scheduled within one week of each other. It was ensured that good hydration was maintained on both scintigraphy days. The dose of either tracer used (^{18}F-NaF or ^{68}Ga-NO2AP-BP) was kept between 111 and 185 MBq (3–5 mCi) and was injected intravenously. After approximately 30 min, the patients were instructed to empty their bladder and thereafter were positioned in supine position with hands by the side on the PET/CT scanner, biograph mCT (Siemens). An initial scan (20 mA,120 kVp) of the whole body was followed by the low dose CT (140 mA, 120 kVp) from vertex to toe, and then the 3D emission scan was acquired at 2 min per bed position for the same landmarks. For dosimetry purpose of ^{68}Ga-NO2AP-BP, we also enrolled five breast cancer patients with suspected skeletal metastases. The detailed pharmacokinetics and dosimetric parameters were undertaken in these five patients.

Analysis and Interpretation

Each study was reconstructed using iterative reconstruction (two iterations, 21 subsets). A multimodality work port (MMWP – Siemens) was used for viewing each study and included the maximum intensity projection image, PET, CT and fused PET/CT images of each tracer. All ^{68}Ga-NO2AP-BP and ^{18}F-NaF images were independently analysed by two nuclear medicine physicians. These physicians were blinded to the results of the ^{99m}Tc-MDP bone scan. The total number of lesions in each patient for ^{68}Ga-NO2AP-BP and ^{18}F-NaF was scored for physician 1 and similarly for physician 2. Each image was also scored visually for quality on the basis of a three-point scale: 1-good quality; 2-moderate quality; 3- poor quality. All foci of abnormal tracer uptake were counted and analysed with respect to their location, SUVmax and characteristic of the lesion on CT; and then classified as benign or metastatic. For calculation of SUVmax, circular regions of interest were drawn around areas with focally increased uptake on transaxial slices.

For dosimetric analysis, all the serial PET/CT scans were conducted in the biograph mCT PET/CT scanner (SIEMENS, Germany). The scan protocol consisted of a scout acquisition, followed by a low dose CT and multiple PET acquisitions at 5, 20, 30, 70, 120 and 240 min post-intravenous injection of an average activity of 159.1 MBq (4.3 mCi) of ^{68}Ga-NO2AP-BP. To maintain uniformity, the time of acquisition of PET images applied per bed was 1 min at all the time points for all patients. Whole blood samples at 5, 15, 30, 60, 80 and 120 min on scanner and urine samples at 50, 160, 180, 220 and 300 min from the time of injection were collected. Whole blood was counted in a scintillation well counter to know the exact amount of activity.

Organs such as liver, right and left kidneys and skeleton were included in the image analysis. Quantification (Bq/ml) for each organ was done using ROI-based method in each slice with automatic thresholding. Whole body counts were taken at respective time points for all the patients. The number of disintegrations (residence times) of the skeleton was based on the measurements determined in ROI around the left humerus. To obtain the values for the whole skeleton, the values were scaled based on the fraction weight that the humerus represents with respect to the whole skeleton. These values were obtained from ICRP 70: 187.4 g for the humerus of one side and 4000 g for the female whole skeleton [13]. Dosimetric calculations were performed using OLINDA/EXM 1.1 software (Organ Level Internal Dose Assessment/Exponential Modelling computer software, Vanderbilt University). The percentage injected activity (%IA) was calculated, in each time point image. Percentage of injected activity was defined as the ratio between the activities in each organ and the injected activity. Values of %IA were entered in the OLINDA software and time activity curves were derived for each organ. The number of disintegrations of each organ was derived from the time activity curves. The blood and urine sample at each time point were counted and decay corrected. The %IA of both blood and urine samples were also entered in

the OLINDA software to derive the number of disintegrations (residence time). The numbers of disintegrations of all the organs were entered in the kinetic input model and the absorbed doses of each organ and whole body effective doses were calculated.

Statistical Methods

Statistical analysis was done using Stata 13 (StataCorp) software package. The agreement analysis regarding number of lesions detected on ^{18}F-NaF and ^{68}Ga-NO2AP-BP was carried out, for which the mean difference between observations with 95 % confidence interval (CI), correlation coefficient, regression coefficient through origin (with 95 % CI) and intraclass correlation coefficient were calculated. A p value of < 0.05 was considered significant.

Results

For the entire study, 28 patients were recruited. In five patients, in addition to lesion detection, dosimetric analysis was performed. For comparison between ^{68}Ga-NO2AP-BP and ^{18}F-NaF, a total of 28 patients were finally included in the study and had ^{68}Ga-NO2AP-BP and ^{18}F-NaF PET/CT performed. Figure 2 shows a comparison of ^{18}F-NaF and ^{68}Ga-NO2AP-BP PET MIP images. There were 27 females and one male patient with pathologically proven breast cancer. The age ranged from 26 years to 67 years (43.8 ± 12.3 years). Referral pattern for bone scintigraphy was as follows: ten patients prior to surgery, one patient after lumpectomy, two patients post-neoadjuvant chemotherapy and 15 patients for post-treatment surveillance. None of the patients received radiotherapy. Histopathologically, 14 patients had infiltrating ductal carcinoma, 13 patients had invasive ductal carcinoma and one patient had invasive lobular carcinoma.

Image quality was graded as good for 26 ^{68}Ga-NO2AP-BP and 27 ^{18}F-NaF studies. There were a total of 199 lesions on consensus reading of both scans, of which 178 lesions were characterised as metastatic and 21 as degenerative/traumatic (Table 1). One patient had a metastatic superscan that was well appreciated on both studies and the patient was excluded from lesion-based analysis (Fig. 3). SUVmax for metastatic lesions on ^{68}Ga-NO2AP-BP and ^{18}F-NaF ranged from 5.2 to 112 (mean = 27.2) to 6.2 to 46.7 (mean = 26.7), respectively (Table 2). Lesion to normal bone ratio ranged from 2.1 to 7.4 (mean = 3.1) for ^{68}Ga-NO2AP-BP and from 2.1 to 6.7 (mean = 3.4) for ^{18}F-NaF (Table 2). Normal bone SUVmax ranged from 4.2 to 39 for ^{68}Ga-NO2AP-BP and 1.3 to 17.7 for ^{18}F-NaF. There was no significant difference found in any of these parameters evaluated on the two studies ($p > 0.05$). Degenerative lesions like osteophytes, facet arthritis and rib fractures showing tracer localisation were noted in five patients on both scans and were correctly interpreted by both physicians using CT correlation. CT demonstrated a total of 187 lesions, among which purely lytic lesions were seen in five patients, predominantly sclerotic lesions in two patients; the remaining lesions were mixed in nature. Both tracers localised in all purely lytic, predominantly sclerotic and lytic/sclerotic lesions. During the study, it was seen that both tracers localised to brain metastases in three patients, which was confirmed on subsequent magnetic resonance imaging [14] and appropriate therapy was instituted. The total number of lesions detected on ^{99m}Tc-MDP in the 27 patients was 150, with 12 degenerative lesions mimicking metastases in one patient.

The number of lesions on ^{68}Ga-NO2AP-BP were correlated between physician 1 and physician 2, and the correlation coefficient was significantly high (r =0.99) (Fig. 4a). Similarly, the number of lesions on ^{18}F-NaF were also correlated between physician 1 and physician 2, and the correlation coefficient was also significantly high (r =0.99) (Fig. 4b). The numbers of lesions detected on ^{68}Ga-NO2AP-BP and ^{18}F-NaF were correlated between both the physicians. The mean difference for number of lesions detected on ^{68}Ga-NO2AP-BP and ^{18}F-NaF was not significant for both the readers, with a high correlation coefficient of 0.99 (Table 3) (Fig. 4c & d). Interobserver regression coefficient was highly significant. Intraclass correlation for both readers was excellent (Table 3).

No adverse reactions to tracer injection was noted on ^{68}Ga-NO2AP-BP studies. The dosimetric analysis showed that the mean doses to kidneys, red marrow, urinary bladder and skeleton were 0.00763 mSv/MBq, 0.0203 mSv/MBq, 0.000113 mSv/MBq and 0.058 mSv/MBq, respectively. The mean whole body effective dose and effective dose equivalent were calculated to be 0.00583 mSv/MBq and 0.0086 mSv/MBq, respectively.

Discussion

The present study revealed excellent correlation in the detection efficiency of metastatic lesions on ^{68}Ga-NO2AP-BP PET/CT when compared to ^{18}F-NaF PET/CT with good localisation in both lytic and sclerotic lesions. All metastatic and degenerative lesions were classified correctly on ^{68}Ga-NO2AP-BP PET/CT. Simultaneous CT acquisition enabled accurate identification of degenerative and traumatic lesions. Although the patient number was small, interobserver correlation, agreement and intraclass correlation was excellent for both studies. Extraskeletal tracer localisation in brain metastases was noted on both studies and reported earlier by us [14]. All three patients were asymptomatic for the same, and subsequent MRI demonstrated cerebral metastases. The possible explanation for extraosseous accumulation of ^{68}Ga-NO2AP-BP includes presence of iron deposits (presence of hemorrhage on MRI), hyperemia or altered capillary permeability of the metastatic lesion. Extraosseous intracranial

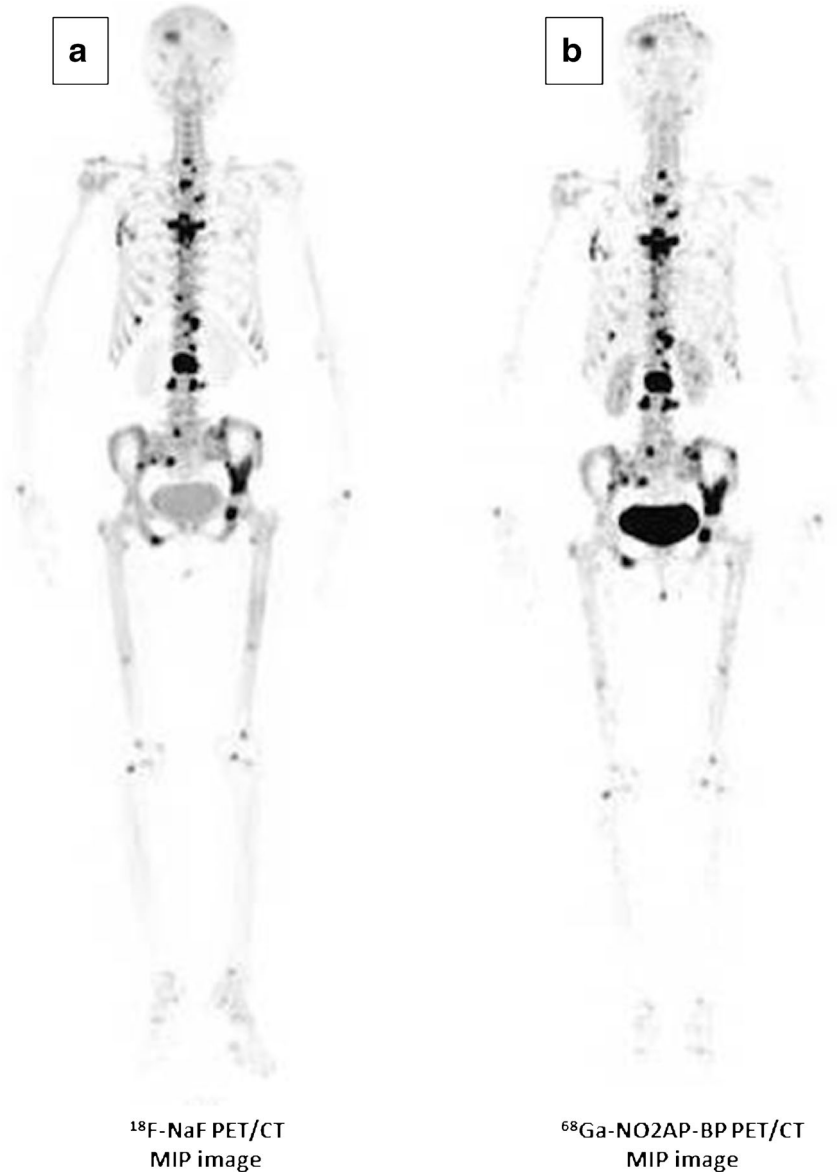

Fig. 2 Figure shows a comparison of ^{18}F-NaF (**a**) and ^{68}Ga-NO2AP-BP (**b**) PET/CT MIP images of a histopathologically proven case of breast carcinoma. Both the scans show increased radiotracer accumulation in skull, multiple cervico-dorsal lumbar vertebrae, multiple bilateral ribs, bilateral pelvic bones, sacrum and bilateral femora

accumulation of conventional bone scintigraphy agent ^{99m}Tc-MDP in metastatic neoplasms has been reported [15]. ^{18}F-NaF has also been reported to accumulate in treated brain metastases [16]. This possibility should be kept in mind while interpreting skeletal PET/CT, as this would facilitate early appropriate management to be instituted.

In vivo experiments have shown that ^{68}Ga-NO2AP-BP has a high binding (93.8 ± 4.4 %) to hydroxyapatite and a fast renal clearance [5]. In addition, ^{68}Ga-NO2AP-BP is taken up by osteoclasts, reflecting the farnesyl diphosphate synthase enzyme dynamics in the HMG-CoA reductase pathway, which may be responsible for a higher detection of lytic lesions [17]. Interestingly, in this study, all purely lytic lesions were detected equally on both ^{18}F-NaF and ^{68}Ga-NO2AP-BP. We could achieve good image quality with acquisition starting at 30 min post-injection at 2 min per bed, 3-D emission scans,

Table 1 Comparison of type of lesions detected on ^{68}Ga-NO2AP-BP PET/CT and ^{18}F-NaF PET/CT by physician 1 and 2

Lesions detected = 199	Physician1 ^{68}Ga-NO2AP-BP	Physician2 ^{68}Ga-NO2AP-BP	Physician1 ^{18}F- NaF	Physician 2 ^{18}F- NaF
Metastatic = 178	168	148	178	169
Degenerative = 21	21	20	21	21
Good scan Quality $N = 28$	26	26	27	27

Fig. 3 Histopathologically proven case of breast carcinoma with metastatic superscan on ^{18}F-NaF and ^{68}Ga-NO2AP-BP PET/CT MIP images

for both ^{68}Ga-NO2AP-BP and ^{18}F-NaF. Similarly, the dose of approximately 111 MBq (3 mCi) resulted in good image quality on both scans.

The effective dose for 25 mCi of ^{99m}Tc-MDP is 5.3 mSv (0.0057 mSv/MBq) [18], and for 5 mCi of ^{18}F-NaF, it is 4.44 mSv (0.024 mSv/MBq) [19]. Thus, for the injected dose of ^{18}F-NaF (185 MBq), the effective dose is in the same range as that of ^{99m}Tc-MDP. The effective dose for ^{68}Ga-NO2AP-BP was calculated to be 0.00583 mSv/MBq; hence, the effective dose for 159.1 MBq (4.3 mCi) of ^{68}Ga-NO2AP-BP is 0.928 mSv. Thus, from all the three skeletal radiotracers, the effective dose estimated for ^{68}Ga-NO2AP-BP was lower by a factor of five than for the two other diagnostic radiopharmaceuticals. The radiation dose to each patient can further be minimised with good hydration and frequent bladder emptying, which we ensured.

The total number of lesions detected on ^{68}Ga-NO2AP-BP and ^{18}F-NaF was more than that on the ^{99m}Tc-MDP scan

Table 2 Comparison of SUVmax of lesions, normal bone and lesion to normal bone ratio between 68Ga-NO2AP-BP PET/CT and 18 F- NaF PET/CT

	^{68}Ga-NO2AP-BP ange (mean)	^{18}F- NaF Range (mean)
SUVmax – metastatic lesions	5.2 to 112 (27.2)	6.2 to 46.7 (26.7)
SUVmax – degenerative lesions	3.3 to 49.1 (25.7)	5.2 to 67.8 (40.3)
SUVmax –normal bone	4.2 to 39 (9)	1.3 to 17.7 (8.1)
Lesion/normal bone ratio	2.1 to 7.4 (3.1)	2.1 to 6.7 (3.4)

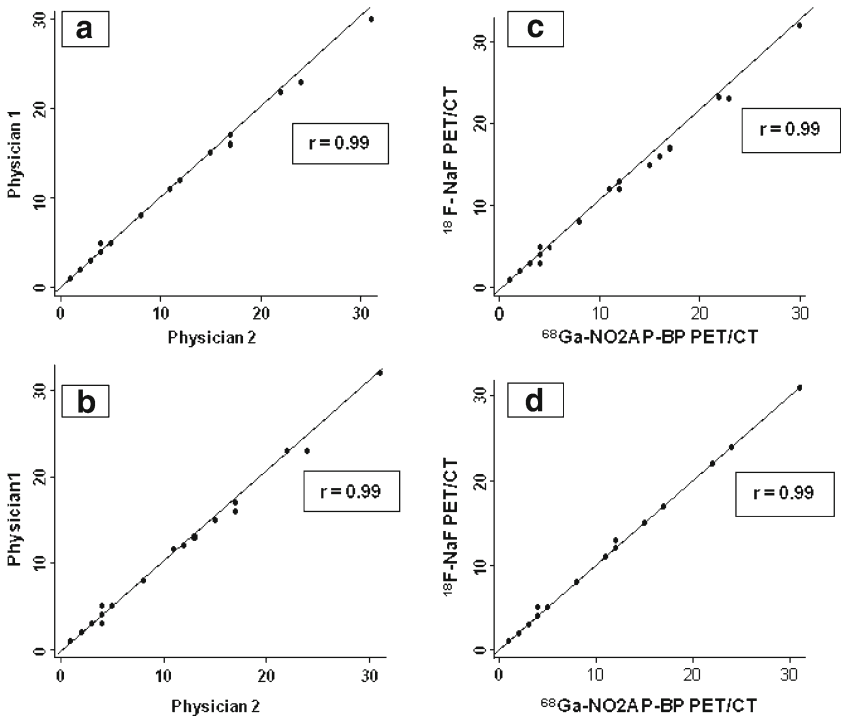

Fig. 4 **a** shows the correlation for number of lesions on ^{68}Ga-NO2AP-BP PET/CT between physician 1 and physician 2, and **b** shows the correlation for number of lesions on ^{18}F-NaF PET CT between physician 1 and physician 2. **c** shows the correlation of number of lesions between ^{18}F-NaF PET CT and ^{68}Ga-NO2AP-BP PET CT for physician 1 and **d** shows the correlation of number of lesions between ^{18}F-NaF PET/CT and ^{68}Ga-NO2AP-BP PET /CT for physician 2

planar and SPECT/CT, again demonstrating the superiority of PET/CT technology over SPECT/CT technology. Degenerative lesions in one patient mimicked metastases on planar imaging because they appeared to be involving the vertebral body, but were clearly identified as degenerative on both ^{68}Ga-NO2AP-BP and ^{18}F-NaF PET/CT. Though SPECT/CT would have also clarified the issue, it was not done in all cases due to technical reasons. The number of lesions detected on ^{68}Ga-NO2AP-BP and ^{18}F-NaF PET/CT ($p = 0.16$) was more than those detected on CT, which reiterates the age-old teaching that radiological lesions in the skeleton are discernible only after at least 30–50 % loss of bone mass.

The DOTA bisphosphonate, BPAMD [4], has also been labelled with ^{68}Ga, resulting in a novel bone seeking radiotracer ^{68}Ga-BPAMD. It has been shown to have faster clearance with high bone to soft tissue ratios [11]. Micro-PET animal experiments have revealed high accumulation of ^{68}Ga-BPAMD in pronounced areas of bone remodelling such as bone metastases [3]. An initial report of its use to image bone metastases in prostate cancer has shown excellent image quality [17]. With the present study we confirm that a triaza-structure of the ^{68}Ga-chelate is also perfectly usable for new ^{68}Ga-macrocyclic bisphosphonate tracers.

The theeoretical prediction that the image quality achieved with ^{68}Ga mono-conjugated bisphosphonate cannot compete with that of ^{18}F-NaF, as ^{18}F possesses a lower positron energy than ^{68}Ga, resulting in lower positron tissue penetration (0.54 mm and 2.12 mm for ^{18}F and ^{68}Ga respectively) and thus lower image blurring, appeared to be not true. As the difference in resolution for a clinical PET scanner is small

Table 3 Correlation of number of lesions in ^{68}Ga-NO2AP-BP PET/CT and ^{18}F- NaF PET /CT between physician 1 (ph 1) and physician 2 (ph 2)

Statistical analysis	^{68}Ga-NO2AP-BP Vs ^{18}F- NaF - ph 1	^{68}Ga-NO2AP-BP Vs ^{18}F-NaF - ph 2	^{68}Ga-NO2AP-BP ph 1 Vs ph 2	^{18}F-NaF ph 1 Vs ph 2
Mean difference	−1.74	−1.44	−1.00	0.37
95 % CI	−0.49 to 0.44	−0.27 to 0.03	−0.27 to 0.09	−2.0 to 3.0
p – value	0.09	0.16	0.32	0.71
Correlation coefficient (r)	0.99	0.99	0.99	0.99
Regression coefficient	1.03	1.00	0.98	1.0
95 % CI	1.01 to 1.05	0.99 to 1.01	0.96 to 0.99	0.98 to 1.02
p-value	0.000	0.000	0.000	0.000
Intraclass correlation	0.999	0.998	0.997	0.999
95 % CI	0.999 – 1.00	0.995 - .999	0.994 to .999	0.997-.999

(3.05 mm for ^{18}F and 3.57 mm for ^{68}Ga), a successful application of ^{68}Ga bone-imaging agents in patients is not precluded [20]. The results of this study agree with these observations and prove the utility of ^{68}Ga-NO2AP-BP for skeletal imaging with equally good results in terms of spatial resolution as for ^{18}F-NaF.

This study validates the utility of ^{68}Ga-NO2AP-BP when compared to ^{18}F-NaF, which is approved by the United States Food and Drug Administration (FDA) and has been the standard agent for skeletal PET/CT till date. ^{18}F-NaF has been shown to be more accurate for detecting skeletal metastases in both breast cancer and prostate cancer patients when compared to ^{99m}Tc-MDP [9]. The ^{68}Ge/^{68}Ga generator produced ^{68}Ga-NO2AP-BP can be an excellent alternative to ^{18}F-NaF. The major advantages perceived with this new agent is that it can be a useful tool for a hospital with PET/CT but without a cyclotron, as it can be conveniently prepared from an onsite ^{68}Ge/^{68}Ga generator system. Moreover, the cost would be similar to that of other PET radiopharmaceuticals. It would also be a useful alternative to ^{99m}Tc-MDP in times of 99Mo-Molybdenum shortage [21]. Its favourable dosimetric data proves its utility from a radiation safety point of view. However, as the study was conducted in a small group of patients, further studies including a greater number of patients and with minor bias need to be conducted.

On a larger prospective, however, the main impact of the ^{68}Ga-bisphosphonates will most probably consist of their theranostic potential. Once the chelated ^{68}Ga-bisphosphonate has identified the patient with localisation of this tracer to nodal and bone metastases, a subsequent therapy with a structural analogue of that bisphosphonate, labelled with trivalent therapeutic radiometal such as ^{177}Lu, will be feasible. This potential application is underway at our centre (FR). However, ^{177}Lu-labelled compounds do not necessarily have biodistribution/pharmacokinetics as 68Ga-labelled radiopharmaceuticals.

Limitations of the study

The limitations of the study are small sample size and a possible referral bias.

Conclusion

Excellent lesion detection between ^{68}Ga-NO2AP-BP PET/CT and ^{18}F-NaF PET/CT with favourable dosimetric results of ^{68}Ga-NO2AP-BP PET/CT suggests the utility of the former as a generator-based PET radiopharmaceutical for skeletal scintigraphy.

Acknowledgement We are grateful to Dr. Chandan J Das for his expertise in reporting the MRI brain scans and Dr. Ganesh Kumar M for keenly reviewing the manuscript. We acknowledge support from Prof. P. Hermann and Dr. V. Kubíček, Charles University in Prague, Czech Republic, for the preparation of NO2AP-BP.

Compliance with ethical standards

Conflict of interest The authors declare that they have no conflict of interest.

Ethical clearance Ethical clearance received Ref. No. IESC/T-236/15.06.2013

Informed consent Informed consent was obtained from all patients.

Funding None.

References

1. Even-Sapir E, Metser U, Mishani E, Lievshitz G, Lerman H, Leibovitch I. The detection of bone metastases in patients with high-risk prostate cancer: ^{99m}Tc-P Planar bonescintigraphy, single- and multi-field-of-view SPECT, ^{18}F-fluoride PET, and ^{18}F-fluoride PET/CT. J Nucl Med. 2006;47:287–97.
2. Yen RF, Chen CY, Cheng MF, Wu YW, Shiau YC, Wu K, et al. The diagnostic and prognostic effectiveness of F-18 sodium fluoride PET-CT in detecting bone metastases for hepatocellular carcinoma patients. Nucl Med Commun. 2010;31:637–45.
3. Fellner M, Biesalski B, Bausbacher N, Kubícek V, Hermann P, Rösch F, et al. ^{68}Ga-BPAMD: PET-imaging of bone metastases with a generator based positron emitter. Nucl Med Biol. 2012;39:993–9.
4. Kubícek V, Rudovský J, Kotek J, Hermann P, Vander Elst L, Muller RN, et al. A bisphosphonate monoamide analogue of DOTA: a potential agent for bone targeting. J Am Chem Soc. 2005;127:16477–85.
5. Holub J, Meckel M, Kubíček V, Rösch F, Hermann P. Gallium(III) complexes of NOTA-bis (phosphonate) conjugates as PET radiotracers for bone imaging. Contrast Media Mol Imaging. 2015;10:122–34.
6. Schirrmeister H, Guhlmann A, Kotzerke J, Santjohanser C, Kühn T, Kreienberg R, et al. Early detection and accurate description of extent of metastatic bone disease in breast cancer with fluoride ion and positron emission tomography. J Clin Oncol. 1999;17:2381–9.
7. Withofs N, Grayet B, Tancredi T, Rorive A, Mella C, Giacomelli F, et al. ^{18}F-Fluoride PET/CT for assessing bone involvement in prostate and breast cancers. Nucl Med Commun. 2011;32:168–76.
8. Iagaru A, Mittra E, Dick DW, Gambhir SS. Prospective evaluation of ^{99m}Tc MDP scintigraphy, ^{18}F NaF PET/CT, and ^{18}F FDG PET/CT for detection of skeletal metastases. Mol Imaging Biol. 2012;14:252–9.
9. Damle NA, Bal C, Bandopadhyaya GP, Kumar L, Kumar P, Malhotra A, et al. The role of ^{18}F-fluoride PET-CT in the detection of bone metastases in patients with breast, lung and prostate carcinoma: a comparison with FDG PET/CT and ^{99m}Tc-MDP bone scan. Jpn J Radiol. 2013;31:262–9.
10. Ibrahim T, Mercatali L, Amadori D. A new emergency in oncology: Bone metastases in breast cancer patients (Review). Oncol Lett. 2013;6:306–10.
11. Zhernosekov KP, Filosofov DV, Baum RP, Aschoff P, Bihl H, Razbash AA, et al. Processing of generator-produced 68Ga for medical application. J Nucl Med. 2007;48:1741–8.

12. Kumar R, Sonkawade RG, Tripathi M, Sharma P, Gupta P, Kumar P, et al. Production of the PET bone agent ^{18}F-fluoride ion, simultaneously with ^{18}F-FDG by a single run of the medical cyclotron with minimal radiation exposure- a novel technique. Hell J Nucl Med. 2014;17:106–10.
13. Basic Anatomical & Physiological Data for use in Radiological Protection - The Skeleton. ICRP Publication 70 - Ann. ICRP 25, 1995.
14. Passah A, Tripathi M, Kumar R, Das CJ, Goyal A, Bal CS. Brain metastasis in carcinoma breast demonstrated on ^{68}Ga NOTA-bisphosphonate PET/CT. Clin Nucl Med. 2014;39:653–4.
15. Sty JR, Starshak RJ, Casper JT. Extraosseous accumulation of Tc-99m MDP. Metastatic intracranial neuroblastoma. Clin Nucl Med. 1983;8:26–7.
16. Tripathi M, Jaimini A, Singh N, Jain N, D'Souza M, Kaur P, et al. F-18 flurodeoxyglucose negative, F-18 fluoride accumulating in a brain metastasis in a treated case of carcinoma of the breast. Clin Nucl Med. 2009;34:287–9.
17. Fellner M, Baum RP, Kubícek V, Hermann P, Luke SL, Prasad V, et al. PET/CT imaging of osteoblastic bone metastases with (68)Ga-bisphosphonates: first human study. Eur J Nucl Med Mol Imaging. 2010;37:834.
18. Wong KK, Piert M. Dynamic bone imaging with 99mTc-labeled diphosphonates and 18F-NaF: mechanisms and applications. J Nucl Med. 2013;54:590–9.
19. Segall G, Delbeke D, Stabin MG, Even-Sapir E, Fair J, Sajdak R, et al. SNM practice guideline for sodium ^{18}F-fluoride PET/CT bone scans 1.0. J Nucl Med. 2010;51:1813–20.
20. Sánchez-Crespo A, Andreo P, Larsson SA. Positron flight in human tissues and its influence on PET image spatial resolution. Eur J Nucl Med Mol Imaging. 2004;31:44–51.
21. Gould P. Medical isotope shortage reaches crisis level. Nature. 2009;460:312–3.